# Synthesis and bioevaluation of $^{125}$I-labeled gold nanorods



2011 Nanotechnology 22 135102

(http://iopscience.iop.org/0957-4484/22/13/135102)

Nanotechnology **22** (2011) 135102 (7pp) doi:10.1088/0957-4484/22/13/135102

# Synthesis and bioevaluation of $^{125}$I-labeled gold nanorods

**Xia Shao[1], Ashish Agarwal[2], Justin R Rajian[1], Nicholas A Kotov[2] and Xueding Wang[1,3]**

[1] Department of Radiology, University of Michigan, Ann Arbor, MI 48109, USA
[2] Department of Chemical Engineering, University of Michigan, Ann Arbor, MI 48109, USA

E-mail: xdwang@umich.edu

Received 14 October 2010, in final form 22 December 2010
Published 22 February 2011
Online at stacks.iop.org/Nano/22/135102

**Abstract**

A novel technique is described for monitoring the *in vivo* behavior of gold nanorods (GNRs) using $\gamma$-imaging. GNRs were radiolabeled using [$^{125}$I] sodium iodide in a simple and fast manner with high yield and without disturbing their optical properties. Radiolabeled GNRs were successfully visualized by radioisotope tagging, allowing longitudinal *in vivo* studies to be performed repeatedly in the same animal. The preliminary biodistribution study showed that PEGylated GNRs have much longer blood circulation times and clear out faster, while bare GNRs accumulate quickly in the liver after systematic administration. The highly efficient method reported here provides an extensively useful tool for guidance of the design and development of new gold nanoparticles as target-specific agents for both diagnostics and photothermal therapy.

(Some figures in this article are in colour only in the electronic version)

## 1. Introduction

Nanoparticles, due to their small sizes and associated unique properties, have been widely used in drug delivery [1–4], cellular imaging [5–9], and biomedical diagnostics and therapeutics [10–13]. Plasmonic gold nanostructures possess intriguing physical and chemical properties which are of interest for both fundamental science and biomedical application [14]. Among the most fascinating and useful are their optical properties as well as related photothermal properties [15]. These optical properties depend on nanoparticle size and shape [16, 17]. One can manipulate the shape of gold nanostructures to control their electronic and associated optical properties for different desired applications [18, 19]. Their remarkable capacity to absorb and scatter light in the visible and near-infrared (NIR) regions is essential for optical imaging [20]. In addition, gold nanoparticles can convert optical energy into heat via nonradiative electron relaxation dynamics which endows them with intense photothermal properties [21–24]. Such localized heating effects can be directed toward the eradication of diseased tissue, providing a noninvasive alternative to surgery [25]. Current nanotechnology research suggests that gold nanoparticles form a novel class of optically active dual imaging–therapeutic agents [26–28].

In particular, gold nanorods (GNRs) have attracted much interest because of their small size, ease of preparation and bioconjugation, strong absorbing and scattering properties, as well as their well-known biocompatibility [14, 20, 29, 30]. GNRs with well-defined shapes and sizes are readily synthesized by seeded growth methods, and their longitudinal plasmon resonances (LPRs) can be finely tuned as a function of aspect ratio [14, 29, 31]. GNRs support a larger absorption cross-section at NIR frequencies per unit volume than most other nanostructures and have narrower line widths due to reduced radiative damping effects with consequently higher optothermal conversion efficiencies [20, 21, 32]. The LPRs can also support nonlinear optical effects, such as plasmon-enhanced two-photon luminescence (TPL) [20, 33]. The LPRs are also sensitive to the polarization of the incident excitation; by slightly adjusting the wavelength of a continuous-wave (cw) polarized laser, individual GNRs can be aligned for several minutes in an optical trap [34]. These properties give rise to many exciting possibilities for deploying GNRs for biological

[3] Author to whom any correspondence should be addressed.

 

imaging and photothermal therapy [20]. Furthermore, the surface chemistry of GNRs allows multiple functionalizations. Capping molecules, such as cetyltrimethylammonium bromide (CTAB), can be replaced or conjugated with many functional groups [35–37]. Target specificity of GNRs can be imparted by tagging with certain biovectors, such as monoclonal antibodies [38], receptor-specific peptides [14], and other compounds [20, 39], which can navigate them to desired organs or sites. Recent studies have successfully demonstrated that GNRs with strong near-IR absorption can be conjugated to molecules to facilitate delivery to the tumor for subsequent efficient cancer cell diagnostics and selective photothermal therapy simultaneously [14, 30, 38].

In addition, the technique of introducing polyethylene glycol (PEG) to the surface of nanoparticles allow steric stabilization of particles. PEG can shield nanoparticles from fouling by serum proteins and reduce the adsorption of reticuloendothelial system (RES) factors in the blood on the particle surface. This reduces the rate of clearance of particles by cells of the monophagocytic system and creates long-circulating particles which hold the promise of *in vivo* utilization of nanoparticles.

To advance GNRs toward realistic clinical applications and to optimize their diagnostic sensitivity, payload, or therapeutic efficiency, it is becoming urgent to understand how they interact with biological systems. Various *in vitro* studies have provided fundamental information as to how nanoparticle size and surface chemistry greatly affect their interaction with plasma proteins, cellular uptake, toxicity, and molecular response. However, the *in vivo* environment is far more complex than *in vitro* model systems [38–41]. For instance, blood contains a variety of ions such as hydrogen, Na, Cl, Ca, etc, as well as proteins, lipids, hydrocarbons, and other components that may affect nanoparticle stability and functionality [38]. Studying the stability and functionality of injected GNRs within the *in vivo* environment is technically challenging.

Recently, there has been increasing use of radioisotopes to study nanoparticles because of the availability of highly sensitive methods to detect radioactivity. In most cases, a bifunctional group, like 1,4,7,10-tetraazadodecane-$N,N',N'',N'''$-tetraacetic acid (DOTA), has to be conjugated to the nanoparticle and then a radioactive metal needs to be attached. This requires modification of nanoparticles before radiolabeling. The study we report here is an initial investigation of the *in vivo* behavior of [$^{125}$I]-iodine-labeled GNRs, which uses I-125 to directly label GNRs. It has been proven that iodide ions show high affinity and strong binding to the surface of GNRs [44–46]. [$^{125}$I]-iodine should be easily tagged onto GNRs by simple mixing. The labeling method developed here can be adapted to $^{123}$I, $^{124}$I, and $^{131}$I for more extensive applications. The stability and metabolism pattern of radiolabeled GNRs in normal rats were successfully examined using $\gamma$-scintigraphy. Longitudinal biodistribution studies have been performed repeatedly in the same animal for up to 6 days, therefore decreasing sources of inter-individual variation while being efficient in terms of animal cost and ethical practice. Radiolabeling of GNRs allows systematic study of gold nanoparticles within *in vitro* and *in vivo* microenvironments, providing a highly efficient methodology for bioevaluation of different kinds of GNRs and their bioconjugates. The novel protocol reported here could be extensively useful for guidance of the design and the development of new target-specific gold nanoparticles.

## 2. Materials and methods

### *2.1. Materials*

[$^{125}$I]radionuclide in $10^{-5}$ M NaOH (pH 8–11) was purchased from PerkinElmer with a specific activity of 100 mCi ml$^{-1}$. Fresh deionized water was used to dilute [$^{125}$I]NaI to the activity desired, around 3 mCi ml$^{-1}$ for animal studies. Chemicals and solvents were purchased from Sigma-Aldrich (Milwaukee, WI, USA) or Fisher Scientific (Fair Lawn, NJ, USA) and used without further purification.

### *2.2. Synthesis of PEGylated GNRs*

GNRs with an average aspect ratio of 4, capped with hexadecyltrimethyl ammonium bromide were synthesized using the seed-mediated growth methods reported in the literature [42, 43]. After synthesis, gold nanorods were centrifuged and re-dispersed in deionized water to a final concentration of $10^{12}$ rods ml$^{-1}$. Polyethylene glycol (PEG) thiol molecules were dispersed in deionized water (1 ml, 50 mg ml$^{-1}$) and mixed with GNRs (1 ml, $10^{12}$ rods ml$^{-1}$). The mixture was allowed to react overnight, followed by centrifugation and re-dispersion of rods to a final concentration of $10^{12}$ rods ml$^{-1}$. The zeta potential of bare GNRs is +40 mV and after PEGylation is reduced to +8 mV (5000 mol. wt) and +10 mV (20 000 mol. wt)

### *2.3. Radiolabeling of GNRs*

In general, 0.1 ml of GNRs with a concentration of $10^{12}$ rods ml$^{-1}$ in deionized water was placed into a polypropylene microcentrifuge tube (1.5 ml) and 0.5 ml of diluted [$^{125}$I]NaI was added, roughly 300 $\mu$Ci of radioactivity. The vial was rotated on a ROTAMIX rotater (Appropriate Technical Resources, Inc. Laurel, MD, USA). The mixture was then centrifuged at 5000 rpm using a Beckman Microfuge II. The supernatant was decanted and pellets were re-dispersed in 0.1 ml of fresh sterile filtered deionized water. Various reaction times of 2, 10, 20, and 30 min were tested, as well as various centrifugation periods of 5, 10, 15, and 30 min. The optical absorption spectra of diluted GNRs in saline solution were measured before and after radiolabeling by using a spectrophotometer (PerkinElmer, MA, USA) with the sample contained in a 1 cm pathlength plastic cuvette. GNRs were also imaged by transmission electron microscopy (TEM).

### *2.4. Stability of GNRs in the blood circulation*

Male Sprague Dawley rats (~250 g) were purchased from Charles River Laboratories (Wilmington, MA, USA). The rats were anesthetized using an isoflurane anesthesia machine. Two

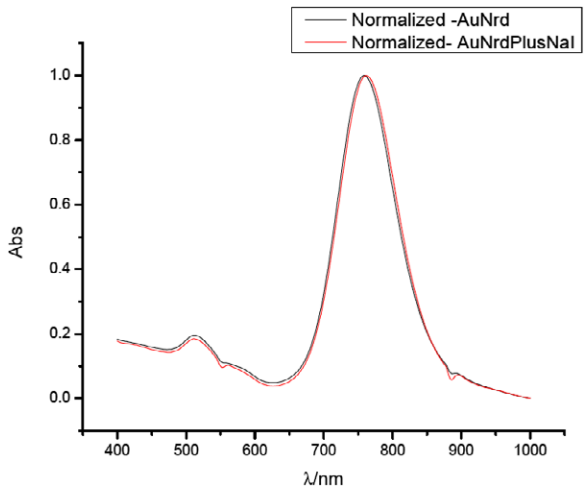


**Figure 1.** UV–vis spectra of GNRs before and after labeling with I-125.

I.V. catheters were placed into lateral tail veins separately, one for injection of the $^{125}$I-GNR dose and another for extraction of blood samples. The catheters were rinsed with 0.2 ml of saline after injection and every extraction. $^{125}$I-labeled GNRs prepared as mentioned above were injected into rats through a tail vein, 100–130 $\mu$Ci in 0.1 ml of water for each animal. Three rats were used for each kind of GNR. Blood samples (0.1 ml) were collected from another tail vein at set times, from 1 min to 4 h post-injection. Radioactivity in each blood sample was counted using a $\gamma$-counter (MINAXI Auto-gamma 5000 series, Packard Instrument Co., Grove, IL, USA).

### *2.5. Long-term biodistribution using $\gamma$-imaging*

The same group of animals used for blood assays were imaged at set times between blood sampling. After the measurements on day 1, the animals were re-anesthetized and scanned once each day from day 2 to day 6 before they were sacrificed. Each image was acquired in 5 min on an anesthetized rat placed in an anterior position over the parallel-hole collimator 1.8/0.2/20 (hole diameter/septum thickness/height in mm) of a Gamma Imager (Biospace Lab, Paris, France). Radioactivity was then quantified by drawing regions of interest (ROIs) using Gamma Vision+ software (Version 3.0). For each animal, ROIs were drawn around the liver/spleen and heart/lung and were saved to be re-used systematically for longitudinal follow-up.

## 3. Results

### *3.1. Preparation of $^{125}$I-labeled GNRs*

GNRs, either bare or PEGylated, were radiolabeled by mixing with [$^{125}$I] sodium iodide in deionized water at room temperature. The reaction takes place very rapidly and completely, with a radiochemical yield greater than 90% by radioactivity count and specific activity greater than $5 \times 10^5$ Ci mmol$^{-1}$. No differences in yield or specific activity were noticed between bare GNRs and PEGylated GNRs. There were no significant differences observed when the mixtures of [$^{125}$I] sodium iodide and GNRs were mixed for 2, 10, 20, or 30 min prior to centrifugation. This agrees well with the prior reports of high affinity and strong binding of iodide ions to the surface of GNRs [44–46]. It has previously been reported that iodide ions may affect the shape and size of GNRs [45]. In our case, the concentration of iodide is extremely low and has no significant impact on the optical property of the GNRs. Figure 1 shows the absorption spectra of GNRs measured before and after radiolabeling in a wavelength range from 400 to 1000 nm. Both transverse and longitudinal plasmon peaks remain unchanged in intensity after radiolabeling but show a small plasmon shift due to the presence of additional iodine molecules on the surface. [$^{125}$I]-iodine-labeled GNRs are stable for weeks when stored in a refrigerator.

**Table 1.** Summary of centrifugation for various periods.

| Total time (min) | Radioactivity in pellets (% from total, $n = 12$) | Aggregation (%) $n = 12$ |
|---|---|---|
| 5 | $60.0 \pm 6.1$ | 0 |
| 10 | $74.4 \pm 3.3$ | 0 |
| 15 | $90.0 \pm 3.1$ | 0 |
| 30 | $99.4 \pm 0.6$ | 33.3 |

The transmission electron microscopy (TEM) images are shown in figure 2. The shape and size of the GNRs remains unchanged before and after radiolabeling. There are no differences observed between bare, 5, and 20 K PEGylated GNRs.

The washing process using centrifugation is critical. Uncompleted centrifugation causes a loss of radioactive GNRs in decanted supernatant, resulting in low radiochemical yields. On the other hand, the chance of irreversible nanorod aggregation increases when the centrifugation period is extended. A series of experiments were performed to investigate and optimize the conditions. To minimize variations, radiolabeled GNRs were initially washed twice to remove free radioactive iodide and then dispersed in deionized water. Table 1 summarizes the percentage of radioactivity collected in pellets after centrifugation for various time periods. It should be noticed that a centrifugation time of 30 min at 5000 rpm is necessary to recover all GNRs. However, the possibility of failure to deliver the desired product would then be over 30% due to irreversible nanorod aggregation. Therefore, one washing using 15 min centrifugation was applied for subsequent animal studies. No further washing will be needed due to the high affinity of iodide ions to GNRs.

In summary, injectable doses for animal studies were prepared by mixing 0.5 ml of [$^{125}$I] sodium iodide with the desired activity and 0.1 ml of GNRs ($10^{12}$ rods ml$^{-1}$) for 5 min, and then centrifuging at 5000 rpm for 15 min. The supernatant was decanted and pellets were re-dispersed in 0.1 ml of fresh sterile filtered deionized water. The same procedure was applied for bare, 5, and 20 K PEGylated GNRs.

### *3.2. Stability of GNRs in the blood circulation*

To determine the circulating time of GNRs, we assayed blood samples from rats ($n = 3$ for each kind of GNR) using $\gamma$-scintigraphy. The time–activity curves are shown in figure 3,

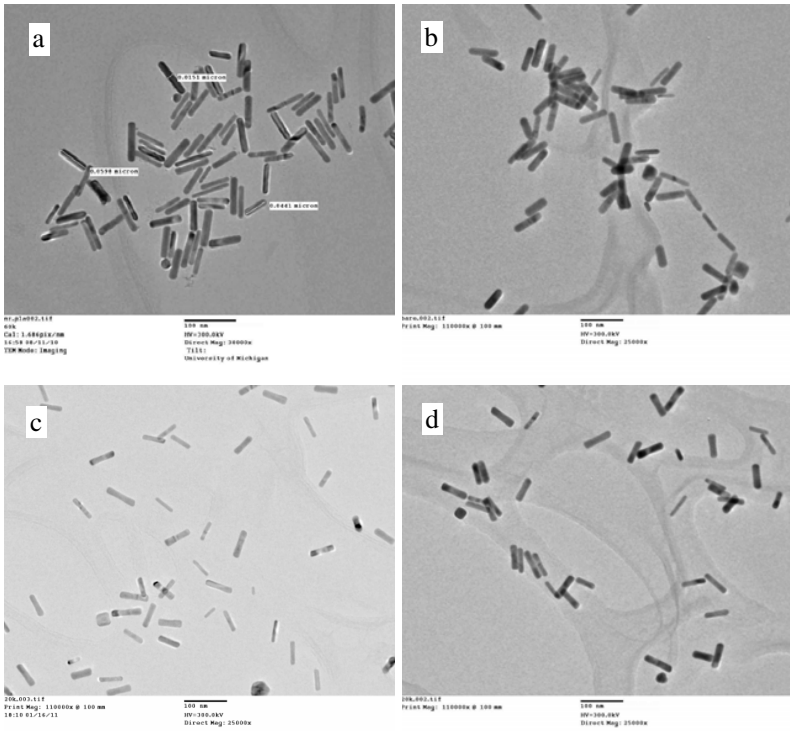


**Figure 2.** TEM images of bare GNRs (a), bare GNRs with I-125 (b), PEGylated GNRs (c) and PEGylated GNRs with I-125 (d).

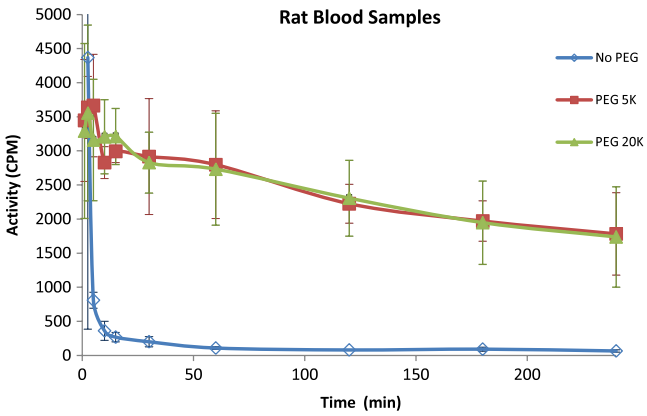


**Figure 3.** Blood time–activity curves.

and indicate significant differences between bare GNRs and PEGylated GNRs. Injected bare GNRs were cleared out from the blood circulation within 10 min, while more than 50% of PEG coated GNRs remained in the blood after 4 h. This is in good agreement with previous studies which have shown that a surface brush layer of PEG reduces the adsorption of blood RES factors to the particle surface, hence decreasing the rate of particle clearance [40, 48]. We have also found that it is irrelevant whether a molecular weight of 5000 or 20 000 is used.

### *3.3. Long-term biodistribution using γ-imaging*

The next experiment evaluated the relatively long-term biodistribution in rats for up to 6 days using $\gamma$-imaging. The same group of animals ($n = 3$ for each kind of GNR) used for blood assays were imaged at set times between blood sampling. Each image was acquired in 5 min on an anesthetized rat placed in an anterior position over the parallel-hole collimator of a Gamma Imager. Radioactivity was then quantified by drawing ROIs. For each animal, ROIs were drawn around the liver/spleen and heart/lung and were saved to be re-used systematically for longitudinal follow-up. Figure 4 shows typical rat gamma images.

The linearity and precision of gamma detection were determined by scanning a series of standards with known radioactivities. The standards were prepared by serial dilution of a $^{125}$I-GNR injection sample. To obtain the average and the standard deviation, each standard was imaged eight times in various positions over the parallel-hole collimator, each taking 5 min for acquisition. Radioactivity was then quantified by drawing ROIs around the standard. Figure 5 shows good correlation between radioactivities counted by a Capintec and radioactivities measured by scintigraphic acquisition of the Gamma Imager. The coefficient of determination ($R^2$ value) was greater than 0.99. The exact position of the sample on the camera head was shown to be irrelevant.

Radioactivities in liver/spleen and heart/lung determined by the Gamma Imager were converted to injection dose based on this standard curve. The uptakes of liver/spleen and heart/lung were then normalized to a percentage of the injected dose for each animal. Results are shown in figure 6.

Uncoated bare GNRs were found to accumulate quickly in the liver and spleen area within 5 min. It should be noted that, for bare GNRs, radioactivity was retained in the liver and spleen for days. The radioactivity well represented the

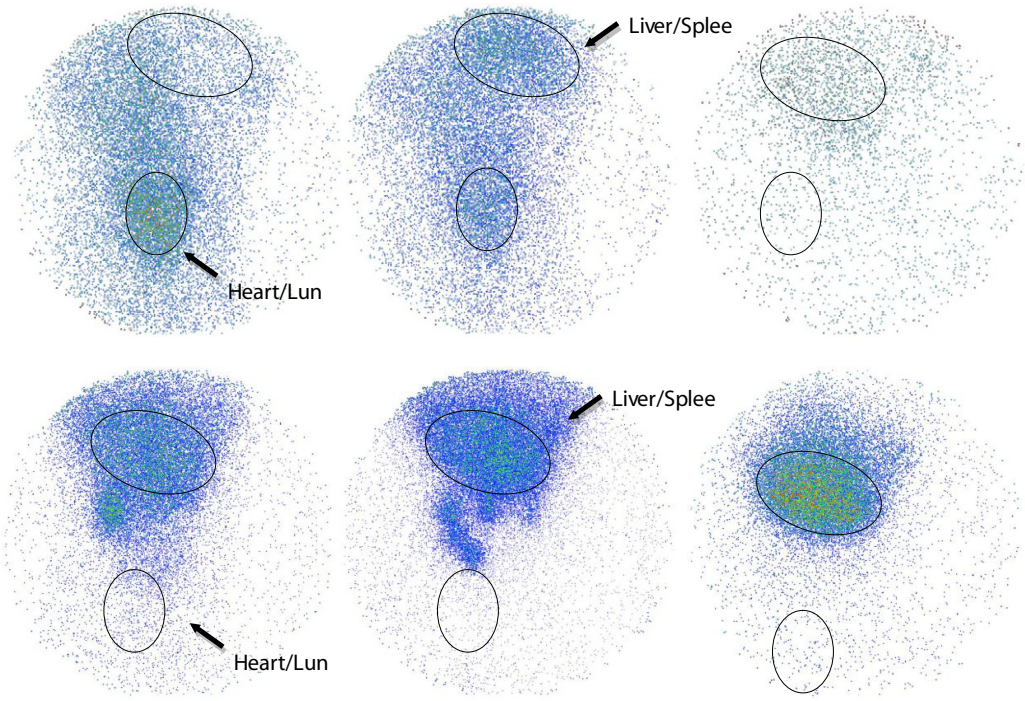


**Figure 4.** Gamma images at different post-injection times (5 min, 4 h, and 6 days). The upper three images are from a rat injected with PEGylated GNRs. The lower three images are from a rat injected with bare GNRs.

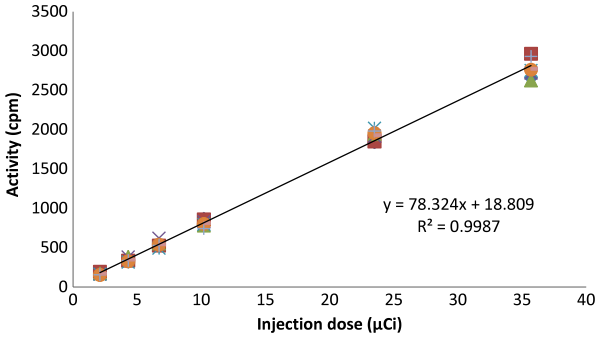


**Figure 5.** $^{125}$I-GNR standard curve.

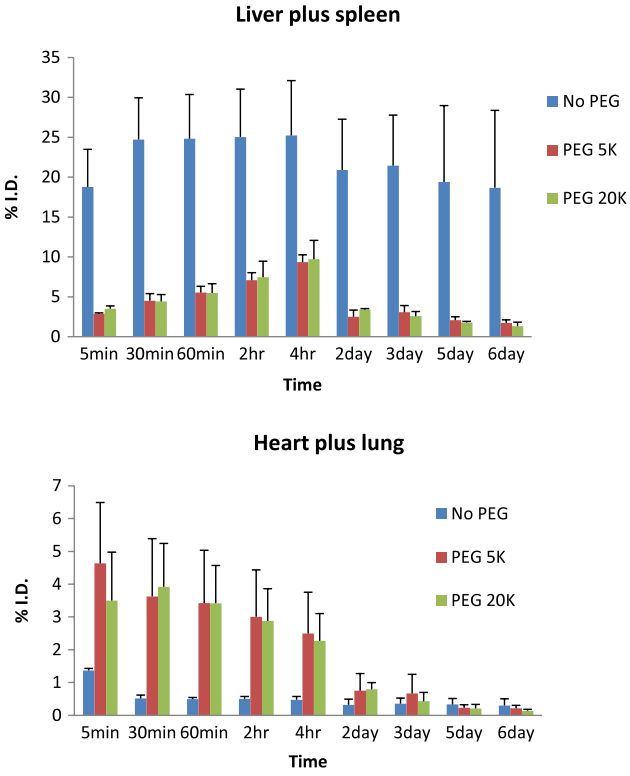


**Figure 6.** Activities in liver/spleen and heart/lung versus time.

concentration of GNRs because any disassociated $^{125}$I should be collected in the thyroid. In contrast, PEG coated GNRs remained in the blood pool for a much longer period, but the long-term accumulation was minimal in the liver and spleen.

All animals were sacrificed at day 6 and examined. There was no apparent damage observed in heart, lung, and liver. Thyroids of all animals had radioactivity as expected. PEG coated GNRs gave a higher thyroid uptake, while bare rods had been trapped in liver tissue from an earlier time point and not much free iodide got into thyroid tissue. To keep all animals in the same condition, we did not pre-treat any rats with cold iodine to block the thyroid in this experiment.

## 4. Discussion

To date, there have been no previously reported *in vivo* animal studies using $^{125}$I-labeled GNRs. We have optimized the radiolabeling procedures, facilitating the reproducible and reliable production of injectable doses for animal studies. GNRs were successfully visualized by a $^{125}$I tag allowing

highly sensitive detection. This simple setup can be further developed to deliver injectable doses for clinical application.

The stability of injected GNRs within the body is a key issue for successful targeting of GNRs because they must be able to circulate in the blood for long enough to find their targets [38]. However, the RES filters nanoparticles from the blood circulation based on their size and surface characteristics [20, 40]. Rapid clearance of nanoparticles from blood limits their targeting capabilities. PEG has well-established 'stealth' properties that can shield nanoparticles from fouling by serum proteins (opsonization) and reduce their rate of clearance by the RES [20, 36]. The beneficial effects of PEGylation on the clearance time of injected nanoparticles have been demonstrated [38, 47]. Therefore, we synthesized three different kinds of GNRs, normal bare GNR, PEGylated GNR with PEG 5000 (mw), and PEG 20 000, and examined their stabilities in the blood circulation. The preliminary animal results are very promising. Significant differences between bare GNRs and PEGylated GNRs have been observed with a minimum number of animals used (figure 3). PEG coated GNRs remained in the blood for much longer than bare GNRs. This provided evidence that a surface brush layer of PEG reduces the adsorption of blood RES factors to the particle surface, hence decreasing the rate of particle clearance [40, 48]. The blood assay method described above is easy and reliable, providing initial information about novel GNRs in biological systems. $\gamma$-Scintigraphy is highly sensitive. Only a low dose of radioactivity has to be administrated and a small amount of blood needs to be drawn for measurement. This simple assay would be the first step for screening any newly designed target-specific GNRs.

The linearity and precision of the Gamma Imager were tested by scanning a series of standards with known radioactivities. The coefficient of determination ($R^2$ value) was greater than 0.99 (figure 5), indicating accurate and reliable measurement. For long-term biodistribution studies, the liver/spleen and heart/lung areas were chosen as ROIs because GNR particles accumulate in the liver and spleen when they are removed from the blood; while they can be seen in the heart and lung when they are still freely circulating in the blood. Figure 6 shows the significant differences in uptakes between bare GNRs and PEGylated GNRs, and more importantly, the distinct pattern of metabolism. The bare GNRs were retained in the liver and spleen for days. This indicates that bare metal particles are cleared from the body with difficulty. In contrast, PEG coated GNRs remained in the blood pool for much longer, but the long-term accumulation was minimal in liver and spleen. For both the measurements from the heart/lung and liver/spleen areas there is no noticeable difference between the results from the GNRs coated with PEG 5000 and PEG 20 000. The observed efficient metabolic clearance pattern provides evidence that PEGylated GNRs are more biocompatible within the body. They are hence ideal candidates for target-specific dual agents for diagnostics and selective photothermal therapy. The trends described here need to be tested in more detail with a wider range of GNRs and will be reported in due course. This methodology provides a highly efficient tool for monitoring *in vivo* behaviors of gold nanoparticles.

In addition, we have successfully utilized GNRs to enhance the contrast in photoacoustic tomography (PAT) [31]. We expect that radioisotope-labeled GNRs can lead to the development of dual-modality imaging with a combination of nuclear imaging modalities, like single photon emission computed tomography (SPECT) or positron emission tomography (PET), and PAT. Furthermore, it is hoped that radiolabeled GNRs will become an efficient therapeutic agent combining the power of radiation therapy and photothermal therapy.

## 5. Conclusion

PEGylated GNRs are ideal candidates for target-specific dual agents for diagnostics and selective photothermal therapy. The methodology developed here should provide a highly efficient protocol for monitoring *in vivo* behaviors of gold nanoparticles. Longitudinal biodistribution studies have been performed repeatedly in the same animal, therefore decreasing sources of inter-individual variations and also being beneficial in terms of animal cost and ethical practice. With this powerful tool in hand, more work can be done to advance GNR technology to a level for clinical use with regard to clearance, safety, efficacy of delivery, and targeting. Encouraged by the preliminary study reported here, further investigations of GNRs of various sizes, shapes, and different conjugates are being investigated. Radiolabeled GNRs hold promise to enable the development of multifunctional nanomedical platforms for simultaneous targeting, imaging, and therapy administration.

## Acknowledgments

This work was supported by National Institutes of Health grant R01 AR055179. We thank Phillip Sherman and Carole Quesada for their assistance with the animal studies.

## References

[1] Rawat M, Singh D and Saraf S 2006 *Biol. Pharm. Bull.* **29** 1790–8
[2] Petrak K 2006 *J. Biomater. Sci. Polym. Edn* **17** 1209–19
[3] Rabinow B and Chaubal M V 2006 *Drugs Pharm. Sci.* **159** 199–229
[4] Chavanpatil M D, Khdair A and Panyam J 2006 *J. Nanosci. Nanotechnol.* **6** 2651–63
[5] Hayat M A and Giaquinta R 1970 *Tissue and Cell* **2** 191–5
[6] Bruchez M Jr, Moronne M, Gin P, Weiss S and Alivisatos A P 1998 *Science* **281** 2016–8
[7] Chan W C and Nie S 1998 *Science* **281** 2016–8
[8] Wu X, Liu H, Liu J, Haley K N, Treadway J A, Larson J P, Ge N, Peale F and Bruchez M P 2003 *Nat. Biotechnol.* **21** 41–6
[9] Sanstra S, Dutta D, Walter G A and Moudgil B M 2005 *Technol. Cancer Res. Treat.* **4** 593–602
[10] Brigger I, Dubernet C and Couvreur P 2002 *Adv. Drug Deliv. Rev.* **54** 631–51
[11] Holm B A, Bergey E J, De T, Rodman D J, Kapoor R, Levy L, Friend C S and Prasad P N 2002 *Mol. Cryst. Liq. Cryst.* **374** 589–98
[12] Moghimi S M, Hunter A C and Murray J C 2005 *FASEB J.* **19** 311–30

[13] Jain K K 2005 *Clin. Chim. Acta* **358** 37–54
[14] Oyeler A K, Chen P C, Huang X, El-Sayed I H and El-Sayed M A 2007 *Bioconjugate* **18** 1490–7
[15] Zhang J Z 2010 *J. Phys. Chem. Lett.* **1** 686–95
[16] El-Sayed M A 2001 *Acc. Chem. Res.* **34** 257–64
[17] Kelly K L, Coronado E, Zhao L and Schatz G C 2003 *J. Phys. Chem.* B **107** 668–77
[18] Sun Y and Xia Y 2002 *Anal. Chem.* **20** 5297–305
[19] Noguez C 2007 *J. Phys. Chem.* B **111** 3806–19
[20] Tong L, Wei Q, Wei A and Cheng J 2009 *Photochem. Photobiol.* **85** 21–32
[21] Chou C-H, Chen C–D and Wang C R C 2005 *J. Phys. Chem.* **109** 11135–8
[22] Petrova H, Juste J P, Pastoriza-Santos I, Hartland G V, Liz-Marzan L M and Mulvaney P 2006 *Phys. Chem. Chem. Phys.* **8** 814–21
[23] Hirsch L R, Stafford R J, Bankson J A, Sershen S R, Rivera B, Price R E, Hazle J D, Halas N J and West J L 2003 *Proc. Natl Acad. Sci. USA* **100** 13549–54
[24] O'Neal D P, Hirsch L R, Halas N J, Payne J D and West J L 2004 *Cancer Lett.* **209** 171–6
[25] Wust P, Hildebrandt B, Sreenivasa G, Rau B, Gellerman J, Riess H, Felix R and Schlag P M 2002 *Lancet Oncol.* **3** 487–97
[26] Chen J, Wang D, Xi J, Au L, Siekkinen A, Warsen A, Li Z Y, Zhang H, Xia Y and Li X 2007 *Nano Lett.* **7** 1318–22
[27] Tong L, Zhao Y, Huff T B, Hansen M N, Wei A and Cheng J–X 2007 *Adv. Mater.* **19** 3136–41
[28] Huff T B, Tong L, Zhao Y, Hansen M N, Cheng J-X and Wei A 2007 *Nanomedicine* **2** 125–32
[29] Niidome T, Akiyama Y, Shimoda K, Kawano T, Mori T, Katayam Y and Niidome Y 2008 *Small* **4** 1001–7
[30] Chanda N, Shukia R, Katti K V and Kannan R 2009 *Nano Lett.*
[31] Chmberland D L, Agarwal A, Kotov N, Fowlkes J B, Carson P L and Wang X 2008 *Nanotechnology* **19** 1–7
[32] Sönnichsen C, Franzl T, Wilk T, von Plessen G and Feld-mann J 2002 *Phys. Rev. Lett.* **88** 077402
[33] Imura K, Nagahara T and Okamoto H 2005 *J. Phys. Chem.* **109** 13214–20
[34] Pelton M, Liu M, Kim H Y, Smith G, Guyot-Sionnest P and Scherer N F 2006 *Opt. Lett.* **31** 2075–7
[35] Liao H and Hafner J H 2005 *Chem. Mater.* **17** 4636–41
[36] Niidome T, Yamagata M, Okamoto Y, Akiyama Y, Takahashi H, Kawan T, Katayama Y and Niidome Y 2006 *J. Control. Release* **114** 343–7
[37] Takahashi H, Niidome Y, Niidome T, Kaneko K, Kawasaki H and Yamada S 2006 *Langmuir* **22** 2–5
[38] Eghtedari M, Liopo A V, Copland J A, Oraevsky A A and Motamedi M 2008 *Nano Lett.* **9** 287–91
[39] Wang C, Chen J, Talavage T and Irudayaraj J 2009 *Angew. Chem. Int. Edn* **48** 2759–63
[40] El Sayed I H, Huang X and El Sayed M A 2005 *Nano Lett.* **5** 829–34
[41] Rouhana L L, Jaber J A and Schlenoff J B 2007 *Langmuir* **23** 12799–801
[42] Carb-Argibay E, Rodrguez-Gonzlez B, Pacifico J, Pastoriza-Santos I, Perez-Juste J and Liz-Marzan L M 2007 *Angew. Chem. Int. Edn* **46** 8983
[43] Perez-Juste J, Pastoriza-Santos I, Liz-Marzan L M and Mulvaney P 2005 *Coordin. Chem. Rev.* **249** 1870
[44] Smith D K, Miller N R and Korgel B A 2009 *Langmuir* **25** 9518–24
[45] Grzelczak M 2008 *Adv. Funct. Mater.* **18** 3780–6
[46] Ha T H, Koo H-J and Chung B H 2007 *J. Phys. Chem.* C **111** 1123
[47] Storm G, Belliot S O, Daemen T and Lasic D D 1995 *Adv. Drug Deliv. Rev.* **17** 31–48
[48] Dunn S E, Brindley A, Davis S S, Davis M C and Illum L 1994 *Pharm. Res.* **7** 1016–22